Trends in rainfall erosivity in NE Spain at annual, seasonal and daily scales, 1955-2006

M. Angulo-Martínez[1] and S. Beguería[1]

[1]{ Department of Soil and Water, Estación Experimental de Aula Dei–Consejo Superior de Investigaciones Científicas (EEAD–CSIC). 1005 Avda. Montañana, 50080–Zaragoza (Spain)}

Correspondence to: S. Beguería (santiago.begueria@csic.es)

Abstract

Rainsplash–the detachment and transport of soil particles by the impact of raindrops on a bare soil–is a major mechanism of soil degradation and erosion on semiarid areas and agricultural lands. Rainfall erosivity refers to the ability of precipitation to erode soil, and depends on characteristics such as total volume, duration, intensity and total energy released by raindrops. Despite the relevance of rainfall erosivity for soil degradation prevention very few studies addressed its spatial and temporal variability. In this study the time variation of rainfall erosivity in the Ebro valley (NE Spain) is assessed for the period 1955–2006. The results show a general decrease in annual and seasonal rainfall erosivity, which is explained by a decrease of very intense rainfall events whilst the frequency of moderate and low events increased. This trend is related to prevailing positive conditions of the main atmospheric teleconnection indices affecting the West Mediterranean, i.e. the North Atlantic Oscillation (NAO), the Mediterranean Oscillation (MO) and the Western Mediterranean Oscillation (WeMO).

1 Introduction

Rainfall erosivity can be defined as the potential of a rainfall event to erode soil, and is a consequence of the interaction of several precipitation characteristics at the event scale. Rainfall erosivity models take account of the continuous and discrete characters of precipitation by considering precipitation amounts and intensities together with the energy

released by raindrops when they hit the soil surface. Individual raindrop impacts are able to detach the soil aggregates and strike them up into the air—rainsplash—, preparing them for being transported by sheet wash or other processes and causing a diffusive displacement of particles down the slope if the topography is not perfectly flat. Rainsplash is also able to disrupt the soil aggregates, and the redistribution of soil particles blocks the soil pores causing crusting and reduced infiltration. Infiltration and saturation excess overland flow may occur as a consequence of the amount and intensity of precipitation over short time periods, causing sheet and concentrated flow with high potential for detaching and transporting soil particles.

The study of rainfall erosivity is thus highly relevant for soil degradation mitigation. Despite its applied relevance, the climatology of rainfall erosivity (i.e. its interannual and seasonal variation, spatial patterns, etc) is surprisingly the topic of very few studies. In the context of climate change, a relevant question is whether or not long-term trends can be detected over the last decades that may help confirming the projections made by global climate models. The Mediterranean basin is one of the areas of the World where current climate projections suggest the highest changes in precipitation (Sauerborn et al., 1999; Kendon et al., 2010; Beaulant et al., 2011; Tramblay et al., 2012). It is expected that the annual precipitation will decrease in the Mediterranean, while higher amounts of erosive rainfall can also be expected as a consequence of changes in precipitation variability and precipitation extremes.

A number of studies found decreasing annual precipitation in the Iberian Peninsula (IP) since the mid 20th century, with seasonal and spatial differences (Rodríguez-Puebla et al., 1998; Esteban-Parra et al., 1998; Paredes et al., 2006; López-Bustins et al., 2008; González-Hidalgo et al., 2009, 2010; Rodrigo, 2010; López-Moreno et al., 20 2010). These trends have been related to changes towards dryer conditions due to a northward displacement of the polar fronts, and are consistent with the evolution of major teleconnection patterns affecting precipitation over the IP such as the North Atlantic Oscillation (NAO), the Mediterranean Oscillation (MO) and the Western Mediterranean Oscillation (WEMO).

Very few studies analyzed trends in rainfall erosivity. Meusburger et al. (2012) analyzed the spatio-temporal variability of rainfall erosivity in Switzerland and found an increasing trend from May to October. Focusing on the Mediterranean side of the IP, de Luis et al. (2010a) found an overall decrease in annual rainfall and increases in rainfall concentration, while changes in rainfall erosivity varied in space. Their analysis was based on the Modified Fournier Index (MFI, Arnoldus, 1977) with monthly precipitation data. This is an important

concern, since rainfall erosivity depends largely on a few number of short but very intense rain episodes that are largely smoothed when data is aggregated at coarser time resolutions.

The USLE/RUSLE *R* factor (Wischmeier, 1959; Wischmeier and Smith, 1978; Brown and Foster, 1987; Renard et al., 1997) is probably the most widely used rainfall erosivity index. It is defined as the mean value of the annual cumulative EI_{30} index. The EI_{30} index (MJ mm ha^{-1} h^{-1}) is obtained for each rainfall event as the product of the kinetic energy of the rain (*E*) and the maximum intensity recorded in 30 min. Its calculation requires high frequency rainfall data – typically one data every 15 min or less –, or pluviograph records. In addition, reliable values of the *R* factor can only be obtained from long data series spanning over several decades. Such conditions are very often not met, so a number of studies have been devoted to estimating rainfall erosivity from coarser data such as highly available daily rainfall time series (Richardson et al., 1983; Bagarello and D'Asaro, 1994; Petkovsek and Mikos, 2004; Angulo-Martínez and Beguería, 2009; Meusburger et al., 2012). Such relationships allow undertaking climatological studies of rainfall erosivity with dense and long datasets. In this article we use an estimation of the EI_{30} index based on daily rainfall intensities for assessing the temporal variation of rainfall erosivity in the NE quadrant of the IP at the annual, monthly and daily time scales.

2 Study area and methods

2.1 Study area

The study area is located at NE of Spain, with an area of about 85,000 km^2 that corresponds to the Ebro River basin (Fig. 1). The area limits to the north with the Cantabric Sea (Atlantic Ocean), the Cantabrian Range and the Pyrenees. Maximum elevations are above 3000 m a.s.l. At the S and SW the Iberian Range closes the Ebro basin, with maximum elevations in the range of 2000–2300 m a.s.l. Catalan Prelitoral Range, with maximum elevations of 1000–1900 m a.s.l. limits the valley to the E, and then continues to the Mediterranean Sea. It is a topographical complex area where mountain areas represent approximately 20% of the study area.

Climate is influenced by the Atlantic Ocean and the Mediterranean Sea, determining a NW–SE climatic gradient. The central area has continental climate with semi-arid conditions as a

consequence of the isolation from the oceanic influence due to topographical shading (Lana and Burgueño 1998). Precipitation is characterized by alternating wet and dry periods as a consequence of the seasonal displacement of the polar front and its associated pressure systems. Drought situations can be followed by torrential rainfall events. Precipitation variability is the main characteristic, inter and intra annually. These properties increase towards the SE and in the center. The most extreme precipitation events are usually recorded along the Mediterranean seaside (Romero et al. 1998 Peñarrocha et al. 2002).

As the rest of climatic variables, rainfall erosivity is characterized by a transition from the NW to the SE (Fig. 2). Three main areas can be recognized: i) the northwest is influenced by the Atlantic Ocean and shows the highest monthly rainfall precipitation with minimum rainfall erosivity, and the highest erosivity is attained coinciding with late spring storms; ii) the central area shows lower precipitation amounts, though erosivity is greater and has two peaks in May–June and August–September; iii) the SE zone has a typical Mediterranean rainfall regime with maxima in spring and autumn, and has the highest erosivities of the study area, especially in autumn.

The main land use in terms of surface is agriculture (representing approximately 46% of the area). It is extended around the Ebro valley occupying a broader area close to the Mediterranean coast. Traditionally, agricultural soils remain uncovered in most cases during autumn and early winter, and as a consequence rainfall erosivity is the main cause of soil erosion during that period.

2.2 Daily rainfall erosivity database

For this study two databases were used (Fig. 1): i) 110 rainfall series from the Ebro river basin authority's hydrologic information system (SAIH Ebro), with a time resolution of 15 minutes since 1997 (P_{SAIH}); and ii) 156 daily rainfall series from the Spanish meteorological agency (AEMET) with daily (0600 to 0600 hours) precipitation amounts for the period 1955-2006 (P_{AEMET}). Precipitation time series were pre-processed with techniques that included reconstruction, gap filling, quality control and homogeneity testing (Vicente-Serrano et al. 2009). The SAIH dataset had the adequate time resolution for computing rainfall erosivity, but only covered eleven years. The AEMET dataset had the adequate length for undertaking climatological studies, but its coarser time resolution did not allow direct computation of the EI_{30} index. Therefore, we used a statistical procedure between the two datasets for obtaining

series of daily rainfall erosivity for the period 1955-2006. The process is explained at length in Angulo-Martínez and Beguería (2009), and a summary is provided as online supplementary material to this article.

Additionally, time series of three widely known teleconnection indices (the North Atlantic Oscillation, NAO; the Mediterranean Oscillation, MO; and the West Mediterranean Oscialltion, WEMO) were used in order to explore atmospheric explanations for the time evolution of rainfall erosivity. Detailed explanation of the elaboration of these time series is provided in Angulo-Martínez and Beguería (2012).

2.3 Trend analysis

Annual and seasonal time series were obtained by adding the daily erosivity values at the appropriate aggregation periods. Natural years (from January 1st to December 31st) were used for the annual series, and the usual convention (winter = December to February, spring = March to May, summer = June to August, autumn = September to November) was used for the seasonal series. In addition, time series of the number of daily erosivity events within the limits of the quintiles of each series (Q1 = below the 20^{th} percentile, Q2 = between the 20^{th} and 40^{th} percentile, Q3 = between the 40^{th} and 60^{th} percentile, Q4 = between the 60^{th} and 80^{th} percentile, Q5 = above the 80^{th} percentile) were computed and aggregated at the annual and seasonal time scales.

The Mann-Kendall test for monotonic trends was used for identifying time trends on those series (Mann, 1945). A block bootstrap procedure was used for obtaining improved significance test when working with time series data (Künsch, 1989). The functions *tsboot* from the R *boot* library and *MannKendall* from the R *Kendall* library were used to perform the analyses. Maps showing the location of the significant series were then produced to help identify possible spatial patterns.

The per-decade change of the annual and seasonal erosivity and the number of events in the first (Q1) and fifth (Q5) quintiles was also represented in the maps to help visualising the sign and magnitude of erosivity trends. Per-decade change was estimated for each series by means of ordinary least squares (OLS) regression upon time, and surface maps were generated by means of local first grade polynomial interpolation.

Relationships between time variation of rainfall erosivity and the three teleconnection indices (NAO, MO and WEMO) were explored by means of the Pearson's correlation test. The number of significantly correlated series was computed for the annual and seasonal erosivity series and for the number of events in the first and fifth quintile. Significance was evaluated at α=0.05 confidence level, so on average a number of n=7.8 false positives could be expected from the 156 time series sample.

3 Results

3.1 Annual and seasonal rainfall erosivity

The annual rainfall erosivity experienced decreasing trends in most of the study area (Fig. 3). Per decade change was as high as -200 MJ mm ha^{-1} h^{-1} y^{-1} in some areas such as in the NE of the study area (eastern Pyrenees), but in most of the area it was lower than 30 MJ mm ha^{-1} h^{-1} y^{-1} per decade. When compared to the mean annual rainfall erosivity (Fig. 2), the highest relative changes occurred at the NE of the study area were they represented 60-80% of the average over the whole study period (five decades).

Spatial differences were most noticeable when analysed at a seasonal basis (Fig. 4). While in winter and spring trends were negative in most of the study area, with the most negative trends in the NE corner, in summer and autumn there were larger spatial differences. Summer yielded the most heterogeneous results, since in some interior areas slightly positive trends were registered while the NE quadrant and some smaller areas in the N and NW experienced strong negative trends. In autumn negative trends predominated overall and were especially strong in the SE and NW corners, but positive trends were also found in the N along the Pyrenean range. Although negative trends predominated overall at both annual and seasonal basis, these results should be taken with care since significance was achieved only in a small fraction of the stations (Table 1).

Variation in the number of events grouped by quintiles allowed assessing trends in the occurrence of rainfall erosivity events across the range of erosivity values (Fig. 5). Since the range of the quintiles were calculated considering the whole study period (1955–2006), negative values indicate a diminishing number of events, while positive values indicate an increasing number of events. The results show that the number of very low and low erosivity

events (Q1, below 20%, and Q2, between 20 and 40%) increased in a large number of stations, while the number of medium, high and very high erosivity events (Q3 to Q5) decreased. Spatially, the number of events in the first quintile increased between one and four events per year in most of the study area, and only in the NE corner (eastern Pyrenees) a negative trend was found (Fig. 6). Trends were significant in the majority of stations (55.8%). The number of events in the fifth quintile, on the other hand, decreased between 0.25 and one event per year, with significant trends in 21.8% of the stations.

The same pattern (increasing number of Q1 events and decreasing number of Q5 events) was found at the seasonal basis (Fig. 7 and 8), with a few exceptions: i) the number of Q1 events decreased in winter in the NE corner; and ii) the number of Q5 events increased in autumn in a small area in the central and western Pyrenees at the N of the study area. The number and proportion of stations with significant trends are shown in Table 2 and Table 3.

The time evolution of the three teleconnection indices is shown in Fig. 9. A tendency towards a prevalence of positive values is clear in the case of the NAO and the MO. Correlations between the time evolution of rainfall erosivity and the teleconnections revealed a high influence of NAO on winter erosivity (43% of the series positively correlated) and autumn (31%), while WEMO and MO had lower influence. With respect to the number of events in the two extreme quintiles, NAO was again the teleconnection with the highest impact, most especially on the evolution of Q5 in winter (44% of positively correlated series).

4 Discussion

Planning of soil conservation measurements, especially concerning agriculture practices, requires a good knowledge of all factors affecting soil erosion. Among them, rainfall erosivity is one of the least studied, although its spatial and temporal dynamics can be of paramount importance when they are related to other factors such as land use and cropping practices. The development of long time series of daily rainfall erosivity, even subject to uncertainty, can be of great value in assessing the spatial and temporal dynamics of rainfall erosivity. Compared to these, data at coarser temporal resolution such as monthly precipitation may miss the importance of a few, very intense events that account for a large fraction of the annual or seasonal rainfall erosivity amounts. Our results show decreasing rainfall erosivities at the annual and seasonal scales over most of the area. This could be explained in part by negative trends in precipitation over the IP especially during the wet season from October to May

(Rodríguez-Puebla et al., 1998; Esteban-Parra et al., 1998; Paredes et al., 2006; López-Bustins et al., 2008; González-Hidalgo et al., 2009, 2010; Rodrigo, 2010; López-Moreno et al., 2010). However, deeper inspection revealed that this trend in the annual erosivity was related to changes in the frequency distribution of erosivity events, since the number of events of low erosivity increased while the number of highly erosive events decreased. Due to the exponential distribution of rainfall erosivity the higher events account for a large part of the total cumulative erosivity, so even a small reduction in the frequency of high events is able to produce a large reduction of the annual or seasonal erosivity. These results are in agreement with previous studies. In their analysis of daily precipitation in the NE of Iberia López-Moreno et al. (2010) found decreasing trends in the number of heavy precipitation events and in the relative contribution of heavy events to the annual rainfall, while the number and relative importance of light and moderate events increased. Similarly, Martínez et al. (2007) described increasing contribution of light and moderate events to total precipitation amounts, and Rodrigo and Trigo (2007) found global decrease in precipitation intensity over the IP. Recent results based on the non-stationary peaks-over-threshold approach to extreme events analysis found evidences of decreasing frequency and magnitude of extreme rainfall events over most of the IP and in particular in its NE quadrant (Beguería et al., 2011; Acero et al., 2012).

Based on monthly precipitation data covering the Mediterranean basins of the IP, de Luis et al. (2010a) reported a generalized decrease of the Modified Fourier Index (MFI). In the Ebro basin, coinciding with the study area of this study, they found that decreasing trends of the MFI predominated in general, except at the N of the study area (Pyrenees). They did not perform seasonal analysis, but in another studies the same authors found that annual and monthly precipitation generally decreased in the Ebro basin except in February and October were a slightly increase was found along the Pyrenees (González-Hidalgo et al., 2009, 2010; de Luis et al., 2010b). This coincides with our findings, since the frequency of high erosivity events (Q5) only increased in autumn in the Pyrenees.

Our results and those of the cited authors contrast with studies for the whole Mediterranean basin, for which a general increase of precipitation intensity has been described (Brunetti et al., 2001; Norrant and Douguédroit, 2006; Goodess and Jones, 2002). However, correlation analysis revealed links with teleconnection patterns that help explain the negative trend in intense precipitation observed in the instrumental records. As other authors pointed out,

strong precipitation events in the study area are significantly related to negative phases of the NAO, MO and WEMO (González-Hidalgo et al., 2009). The generalized decreasing precipitation along the Mediterranean basin of the IP has been related to prevailing positive conditions of NAO and MO. Angulo-Martínez and Beguería (2012) found a significant relationship between rainfall erosivity and these indices, which was largest for MO and WEMO. These authors related the positive trend of these indices with the observed reduction in the occurrence of extreme rainfall events. Similar results were obtained by Vicente-Serrano et al. (2009) with respect to extreme precipitation in NE Spain. Here we found that a high number of rainfall erosivity series were correlated with the time evolution of NAO, most especially in winter and autumn, and that the reduction in the number of erosivity events in the fifth quintile was also related to the NAO.

5 Conclusions

Analysis of the temporal evolution of rainfall erosivity revealed generalized decreasing trends at the annual and monthly scales during the period 1955–2006, coinciding with a decrease in the number of highly daily erosive events and increasing number of daily low erosivity events. These trends could be explained by the displacement of the polar fronts northwards revealed by the positive trend of the NAO and MO.

This study reveals that rainfall erosivity is characterized by complex patterns in time and space, but their study can be undertaken based on relatively common data (long time series of daily precipitation and shorter time series of high frequency precipitation). This encourages the climatological study of this rainfall property, given the implications for soil erosion and the hydrological behavior on natural and managed landscapes.

Acknowledgements

We want to express our gratitude to the Spanish Meteorological Agency (Agencia Española de Meteorología, AEMET) and the Ebro Basin Water Authority (Confederación Hidrográfica del Ebro, CHE) for providing the data used in this study. This work has been supported by research projects CGL2011–24185 financed by the Spanish Ministry of Science and Innovation (CICYT) and the European Regional Development Fund (ERDF—FEDER), 2010CZ0021 financed by the Spanish National Research Council (Consejo Superior de

Investigaciones Científicas—CSIC) and the Czech Academy of Sciences, and 'Grupo de Investigación E68: Geomorfología y Cambio Global' financed by the Aragón Government and the European Social Fund (ESF—FSE). Research of M. A.-M. was supported by a JAE-Predoc grant from the Spanish National Research Council (Consejo Superior de Investigaciones Científicas—CSIC).

References

Acero, J.L., García, J.A., Gallego, M.C.: Peaks-over-Threshold Study of Trends in Extreme Rainfall over the Iberian Peninsula, J. Climate, 24, 1089–1105, 2012.

Angulo-Martínez, M., Beguería, S.: Do atmospheric teleconnection patterns influence rainfall erosivity? A comparison between NAO, MO and WeMO in NE Spain, 1955-2006, J. Hydrol., doi:10.1016/j.jhydrol.2012.04.063

Angulo-Martínez, M., Beguería, S.: Evaluation of the Relationship Between the NAO and Rainfall Erosivity in NE Spain During the Period 1955–2006. Advances in Global Change Research, 46, 183-197, 2011.

Angulo-Martínez, M., Beguería, S.: Estimating rainfall erosivity from daily rainfall records: A comparison among methods using data from the Ebro Basin (NE Spain). J. Hydrol., 379, 111-121, 2009.

Angulo-Martínez, M., Beguería S. Do atmospheric teleconnection patterns influence rainfall erosivity? A comparison between NAO, MO and WEMO in NE Spain, 1955-2006. J. Hydrol., **450-451**, 168–179, 2012.

Arnoldus, H.M.J.: Methodology used to determine the maximum potential average annual soil loss due to sheet and rill erosion in Morocco. FAO Soils Bull., 34, 39-51, 1977.

Bagarello, V., D'Asaro, F.: Estimating single storm erosion index. T. ASAE, 37, 785-791, 1994.

Beaulant, A.L., Joly, B., Nuissier, O., Somot, S., Ducrocq, V., Joly A., Sevault, F., Deque, M., Ricard, D.: Statistico-dynamical downscaling for Mediterranean heavy precipitation. J. Roy. Meteor. Soc., 137, 736–748, 2011.

Beguería, S., Angulo-Martínez, M., Vicente-Serrano, S. M., López-Moreno, J.I., El-Kenawy, A.: Assessing trends in extreme precipitation events intensity and magnitude using non-

stationary peaks-over-threshold analysis: a case study in northeast Spain from 1930 to 2006. Int. J. Climatol., 31, 2102–2114, 2011.

Brown, L.C., Foster, G.R.: Storm erosivity using idealized intensity distributions. T. ASAE., 30, 379-386, 1987.

Brunetti M, Maugeri M, Nanni T. 2001. Changes in total precipitation, rainy days and extreme events in northeastern Italy. Int. J. Climatol. **21**: 861–871.

de Luis, M., González-Hidalgo, J.C., Longares, L.A.: Is rainfall erosivity increasing in the Mediterranean Iberian Peninsula? Land Degrad Dev, 21, 139-144, 2010a.

de Luis, M., Brunetti, M., González-Hidalgo, J.C., Longares, L.A., Martín-Vide, L.A.: Changes in seasonal precipitation in the Iberian Peninsula during 1946–2005. Global Planet. Change, 74, 27–33, 2010b.

D'Odorico, P., Yoo, J., Over, T.M.: An assessment of ENSO-Induced patterns of rainfall erosivity in the Southwestern United States. J. Climate, 14, 4230-4242, 2001.

Esteban-Parra, M.J., Rodrigo, F.S., Castro-Díez, Y.: Spatial and temporal patterns of rainfall in Spain for the period 1880–1992. Int. J. Climatol., 18, 1557–1574, 1998.

González-Hidalgo, J.C., Brunetti, M., de Luis, M.: Precipitation trends in Spanish hydrological divisions, 1946–2005. Clim. Res., 43, 215–228, 2010.

González-Hidalgo, J.C., Lopez-Bustins, J.A., Štepánek, P., Martín-Vide, J., de Luis, M.: Monthly rainfall trends on the Mediterranean fringe of the Iberian peninsula during the second-half of the twentieth century (1951-2000). Int. J. Climatol., 29, 1415-1429, 2009.

Goodess CM, Jones PD. 2002. Links between circulation and changes in the characteristics of Iberian rainfall. Int. J. Climatol. **22**: 1593–1615.

Kendon, E.J., Rowell, D.P., Jones, R.G.: Mechanisms and reliability of future projected changes in daily rainfall. Clim. Dynam., 35, 489-509, 2010.

Künsch, H.R. 1989. The jacknife and the bootstrap for general stationary observations. Annals of Statistics, **17**, 1217–1241.

Lana, X., Burgueño, A.: Spatial and temporal characterization of annual extreme droughts in Catalonia (Northeast Spain). Int. J. Climatol., 18, 93–110, 1998.

Lopez-Bustins, J.A., Martin-Vide, J., Sanchez-Lorenzo, A.: Iberia winter rainfall trends based upon changes in teleconnection and circulation patterns. Global Planet. Change, 63, 171-176, 2008.

López-Moreno, J.I., Vicente-Serrano, S. M., Angulo-Martínez, M., Beguería, S., El-Kenawy, A.: Trends in daily precipitation on the north eastern Iberian Peninsula, 1955–2006. Int. J. Climatol., 30, 1026–1041, 2010.

Mann, H.B. 1945. Nonparametric tests against trend. Econometrica, **13**: 245–259.

Martínez MD, Lana X, Burgueño A, Serra C. 2007. Spatial and temporal daily rainfall regime in Catalonia (NE Spain) derived from four precipitation indices, years 1950–2000. Int. J. Climatol., **27**: 1527–1632.

Meusburger, K., Steel, A., Panagos, P., Montanarella, L., Alewell, C. Spatial and temporal variability of rainfall erosivity factor for Switzerland, Hydrol. Earth Syst. Sci., 16, 167–177, 2012.

Nearing, M.A., Pruski, F.F., O'Neal, M.R.: Expected climate change impacts on soil erosion rates: A review. J. Soil Water Conserv., 59, 1, 43-50, 2004.

Norrant C, Douguédroit A. 2006. Monthly and daily precipitation trends in the Mediterranean (1950–2000). Theor. Appl. Climatol. **83**: 89–106.

Paredes, D., Trigo, R.M., García-Herrera, R., Franco-Trigo, I.: Understanding rainfall changes in Iberia in early spring: weather typing and storm-tracking approaches. J. Hydrometer., 7, 101-113, 2006.

Peñarrocha, D., Estrela, M.J., Millán, M.: Classification of daily rainfall patterns in a Mediterranean area with extreme intensity levels: the Valencia region. Int. J. Climatol., 22, 677–695, 2002.

Petkovsek, G., Mikos, M.: Estimating the R factor from daily rainfall data in the sub-Mediterranean climate of southwest Slovenia. Hydrolog. sci. j., 49 (5), 869-877, 2004.

Renard, K.G., Foster, G.R., Weesies, G.A., McCool, D.K., Yoder, D.C.: *Predicting Soil Erosion by Water: A Guide to Conservation Planning with the Revised Universal Soil Loss Equation (RUSLE)*. Handbook #703. US Department of Agriculture, Washington, DC, 1997.

Richardson, C.W., Foster, G.R., Wright, D.A.: Estimation of Erosion Index from Daily Rainfall Amount. T. ASAE, 26, 153-160, 1983.

Rodrigo, F.S.: Changes in the probability of extreme daily precipitation observed from 1951 to 2002 in the Iberian Peninsula. Int. J. Climatol., 30, 1512–1525, 2010.

Rodrigo FS, Trigo RM. 2007. Trends in daily rainfall in the Iberian Peninsula from 1951 to 2002. Int. J. Climatol. **27**: 513–529.

Romero, R., Guijarro, J.A., Ramis, C. and Alonso, S.: A 30-year (1964-1993) daily rainfall data base for the Spanish Mediterranean regions: first exploratory study. Int. J. Climatol., 18, 541-560, 1998.

Sauerborn, P., Klein, D.A., Botschek, J., Skowronek, A.: Future rainfall erosivity from large scale climate models – methods and scenarios for a humid region. Geoderma., 93, 269-276, 1999.

Tramblay, Y., Badi, W., Driouech, F., El Adlouni, S., Neppel, L., Servat, E.: Climate change impacts on extreme precipitation in Morocco. Global Planet. Change. 82–83, 104–114, 2012.

Vicente-Serrano, S.M., Beguería, S., López-Moreno, J.I., García-Vera, M.A., Stepanek, P.: A complete daily rainfall database for north-east Spain: Reconstruction, quality control and homogeneity. Int. J. Climatol, 30, 1146-1163, 2009.

Vicente-Serrano, S.M., Beguería, S., López-Moreno, J.I., El Kenawy, A., Angulo-Martínez, M. Daily atmospheric circulation events and extreme precipitation risk in northeast Spain: Role of the North Atlantic Oscillation, the Western Mediterranean Oscillation, and the Mediterranean Oscillation. Journal of Geophysical Research, 114, D08106, doi:10.1029/2008JD011492, 2009.

Wischmeier, W.H., Smith, D.D.: Predicting rainfall erosion losses: a guide to conservation planning. *USDA Handbook 537,* Washington, DC, 1978.

Wischmeier, W.H.: A rainfall erosion index for a universal soil-loss equation. Soil Sci. Soc. Amer. Proc., 23, 246-249, 1959.

1 Table 1: Number and proportion of series with significant trends, significance level α=0.05.

Time period	Nº positive trends (%)	Nº negative trends (%)
Annual	1 (0.6%)	23 (14.7%)
Spring	1 (0.6%)	8 (5.1%)
Summer	0	9 (5.8%)
Autumn	1 (0.6%)	3(1.9%)
Winter	0	25 (16.0%)

2

3 Table 2. Number and proportion of series with trends in the number of events in the first
4 quintile (Q1), significance level α=0.05.

Time period	Nº positive trends (%)	Nº negative trends (%)
Annual	72 (46.2%)	15 (9.6%)
Spring	59 (37.8%)	11 (7.1%)
Summer	54 (34.6%)	11 (7.1%)
Autumn	81 (51.9%)	7 (4.5%)
Winter	54 (34.6%)	15 (9.6%)

5

6 Table 3. Number and proportion of series with trends in the number of events in the fifth
7 quintile (Q5), significance level α=0.05.

Time period	Nº positive trends (%)	Nº negative trends (%)
Annual	0	34 (21.8%)
Spring	1 (0.6%)	6 (3.9%)
Summer	0	23 (14.7%)
Autumn	1(0.6%)	9 (5.8%)
Winter	0	28 (21.8%)

8

Table 4. Number of significant correlations between atmospheric circulation indices and rainfall erosivity (Pearson's correlation test, significance level α=0.05).

	Annual	DJF	MAM	JJA	SON
Erosivity (EI)					
NAO_i	13 (8.3%)	67 (43%)	0	6 (3.9%)	49 (31.4%)
$WEMO_i$	8 (5.1%)	20 (12.8%)	3 (1.9%)	1 (0.6%)	10 (6.4%)
MO_i	13 (8.3%)	7 (4.5%)	2 (1.9%)	27 (17.3%)	8 (5.1%)
Nº of daily erosivity events in the first quintile (Q1)					
NAO_i	18 (11.5%)	23 (14.7%)	17 (11%)	11 (7.1%)	25 (16%)
$WEMO_i$	10 (6.4%)	12 (8%)	10 (6.4%)	8 (5.1%)	11 (7.1%)
MO_i	16 (12.2%)	9 (5.8%)	7 (4.5%)	28 (18%)	3 (1.9%)
Nº of daily erosivity events in the fifth quintile (Q5)					
NAO_i	2 (1.9%)	68 (44%)	2 (1.9%)	3 (1.9%)	39 (25%)
$WEMO_i$	19 (12.2%)	20 (12.8%)	3 (1.9%)	4 (2.6%)	11 (7.1%)
MO_i	20 (12.8%)	15 (9.6%)	4 (2.6%)	29 (18.6%)	3 (1.9%)

Figure 1. Digital Terrain Model of the study area showing the spatial distribution of the rainfall gauges used in the study (UTM coordinates). P_{AEMET} indicates daily rainfall data series for period 1955-2006 provided by the Spanish Meteorological Agency. P_{SAIH} indicates the 15' rainfall data series for period 1997-2006 provided by the Automatic Hydrologic Information System of the Ebro river basin.

Figure 2. Mean annual rainfall erosivity during the period 1955-2006 (MJ mm ha^{-1} h^{-1} y^{-1}).

Figure 3. Per decade change of annual rainfall erosivity during the period 1955-2006 (MJ mm ha^{-1} h^{-1} y^{-1}). Black circles indicate data series for which the trend was significant at the α=0.05 confidence level.

Figure 4. Per decade change of seasonal rainfall erosivity during the period 1955-2006 (MJ mm ha^{-1} h^{-1} y^{-1}): a) DJF, b) MAM, c) JJA, d) SON. Black circles indicate data series for which the trend was significant at the α =0.05 confidence level.

Figure 5. Boxplots of trends with the number of daily rainfall erosivity events classified by quintiles of daily erosivity over the whole period 1955-2006.

Figure 6. Per decade change in the number of daily rainfall erosivity events corresponding to a) the first (Q1) and b) fifth (Q5) quintiles at the annual scale for the period 1955-2006. Black circles indicate significant trends at the α =0.05 confidence level.

Figure 7. Per decade change in the number of daily rainfall erosivity events corresponding to the first (Q1) quintile at the seasonal scale for the period 1955-2006: a) DJF, b) MAM, c) JJA, d) SON. Black circles indicate significant trends at the α =0.05 confidence level.

1 Figure 8. Per decade change in the number of daily rainfall erosivity events corresponding to
2 the fifth (Q5) quintile at the seasonal scale for the period 1955-2006: a) DJF, b) MAM, c)
3 JJA, d) SON. Black circles indicate significant trends at the α =0.05 confidence level.

4

5 Figure 9. Temporal evolution of October to March NAO, WeMO and MO indices obtained
6 from average daily indices (thin black line) and 5-years running average (thick grey line).

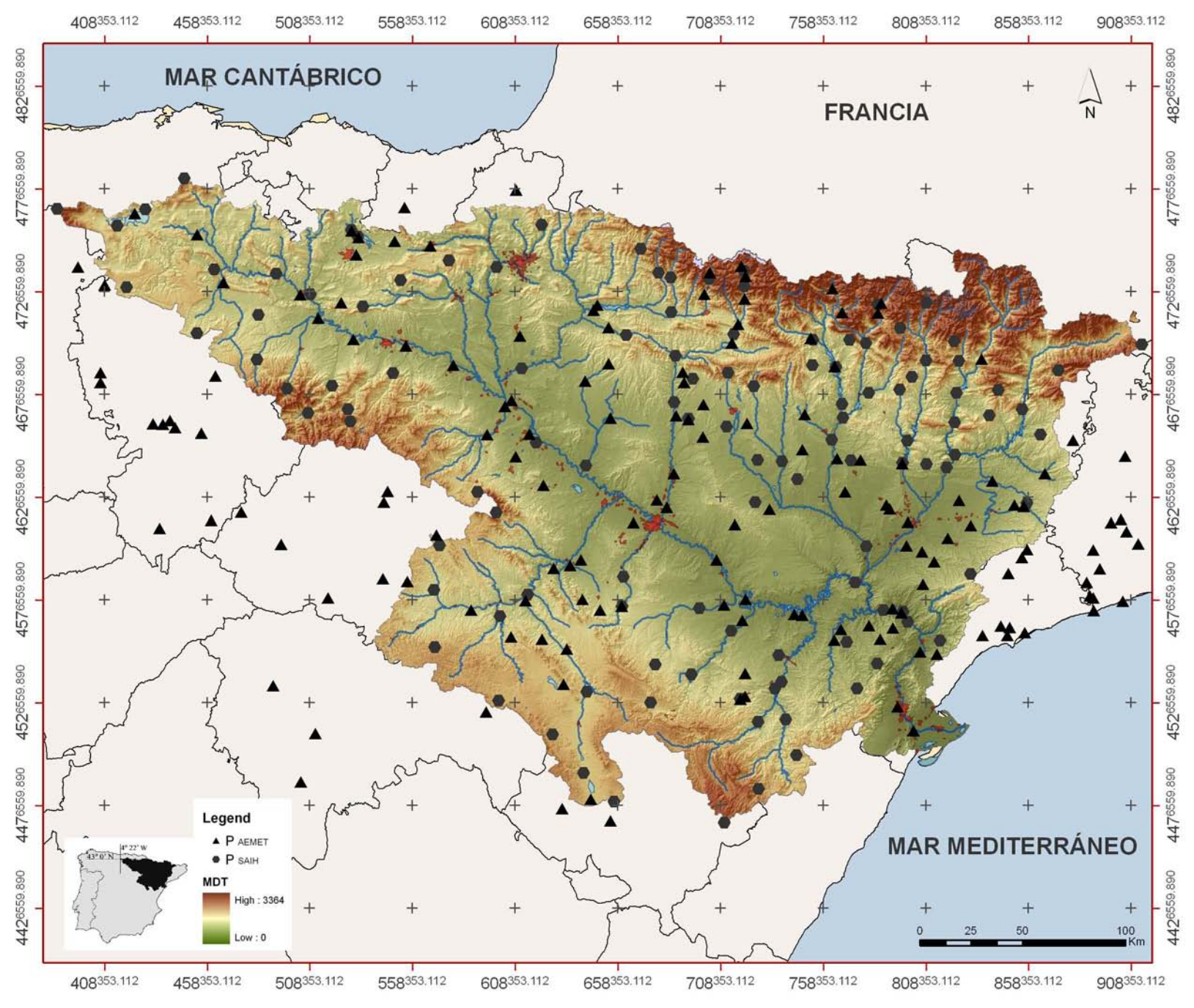
MAR CANTÁBRICO
FRANCIA
N
MAR MEDITERRÁNEO
Legend
P AEMET
P SAIH
MDT
High : 3364
Low : 0
0 25 50 100
Km
408353.112
458353.112
508353.112
558353.112
608353.112
658353.112
708353.112
758353.112
808353.112
858353.112
908353.112
4826559.890
4776559.890
4726559.890
4676559.890
4626559.890
4576559.890
4526559.890
4476559.890
4426559.890

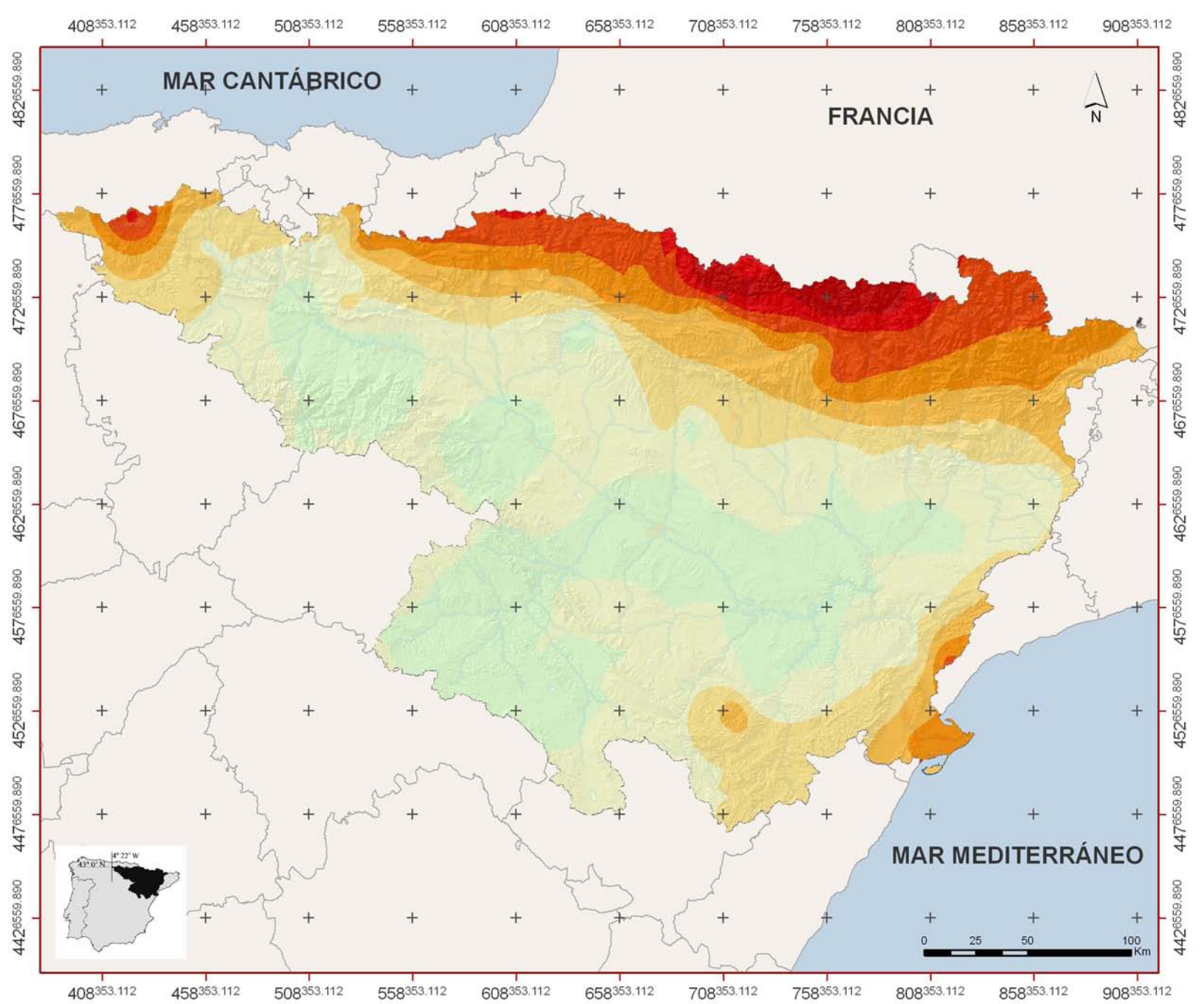

Erosividad media anual

1955-2006; (MJ mm ha^{-1} h^{-1} y^{-1})

300 - 500	700 - 900	1100 - 1300	1600 - 1900
500 - 700	900 - 1100	1300 - 1600	1900 - 2700

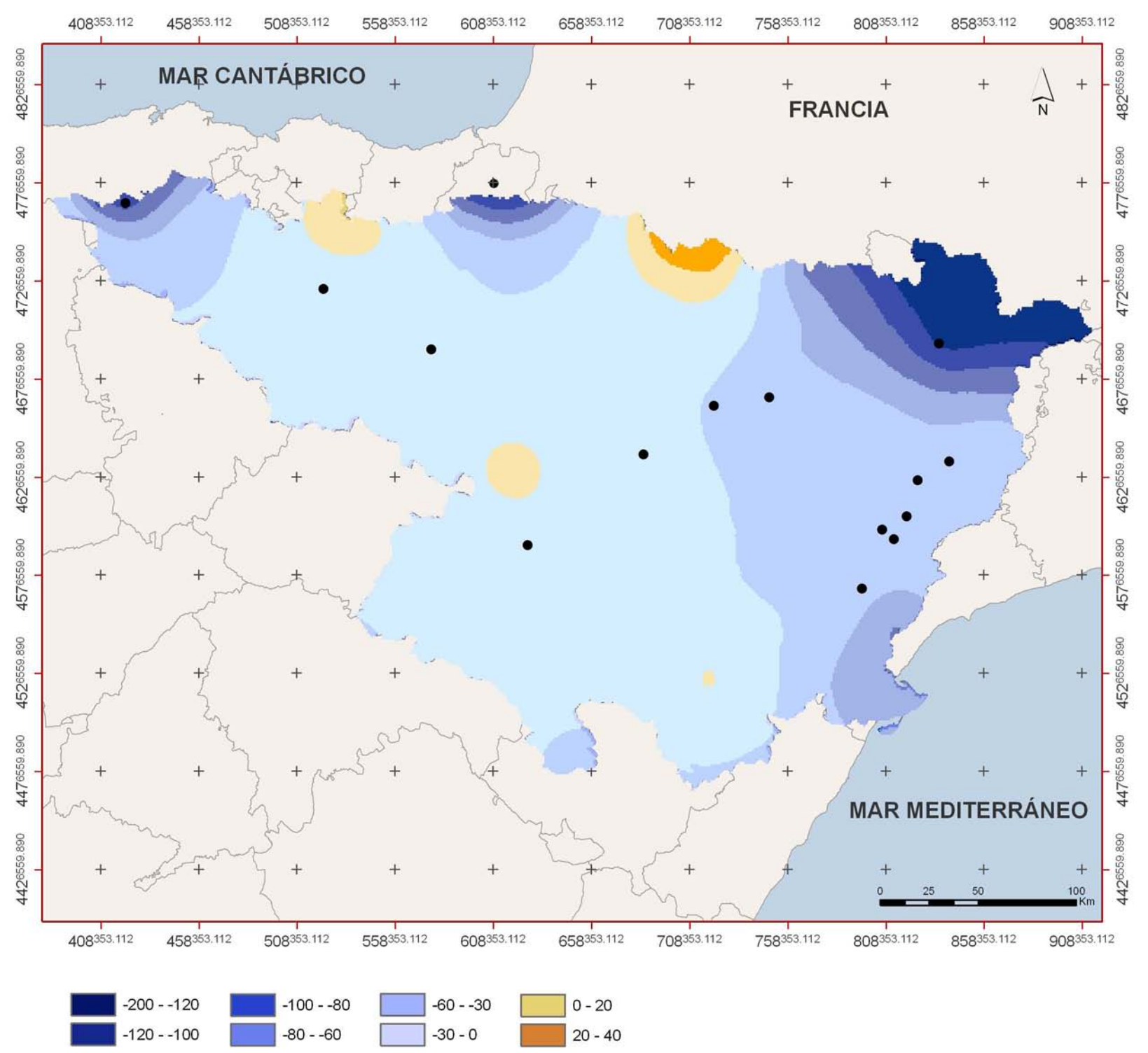
MAR CANTÁBRICO
FRANCIA
MAR MEDITERRÁNEO
N
0 25 50 100
Km
408353.112
458353.112
508353.112
558353.112
608353.112
658353.112
708353.112
758353.112
808353.112
858353.112
908353.112
4826559.890
4776559.890
4726559.890
4676559.890
4626559.890
4576559.890
4526559.890
4476559.890
4426559.890
-200 - -120
-120 - -100
-100 - -80
-80 - -60
-60 - -30
-30 - 0
0 - 20
20 - 40

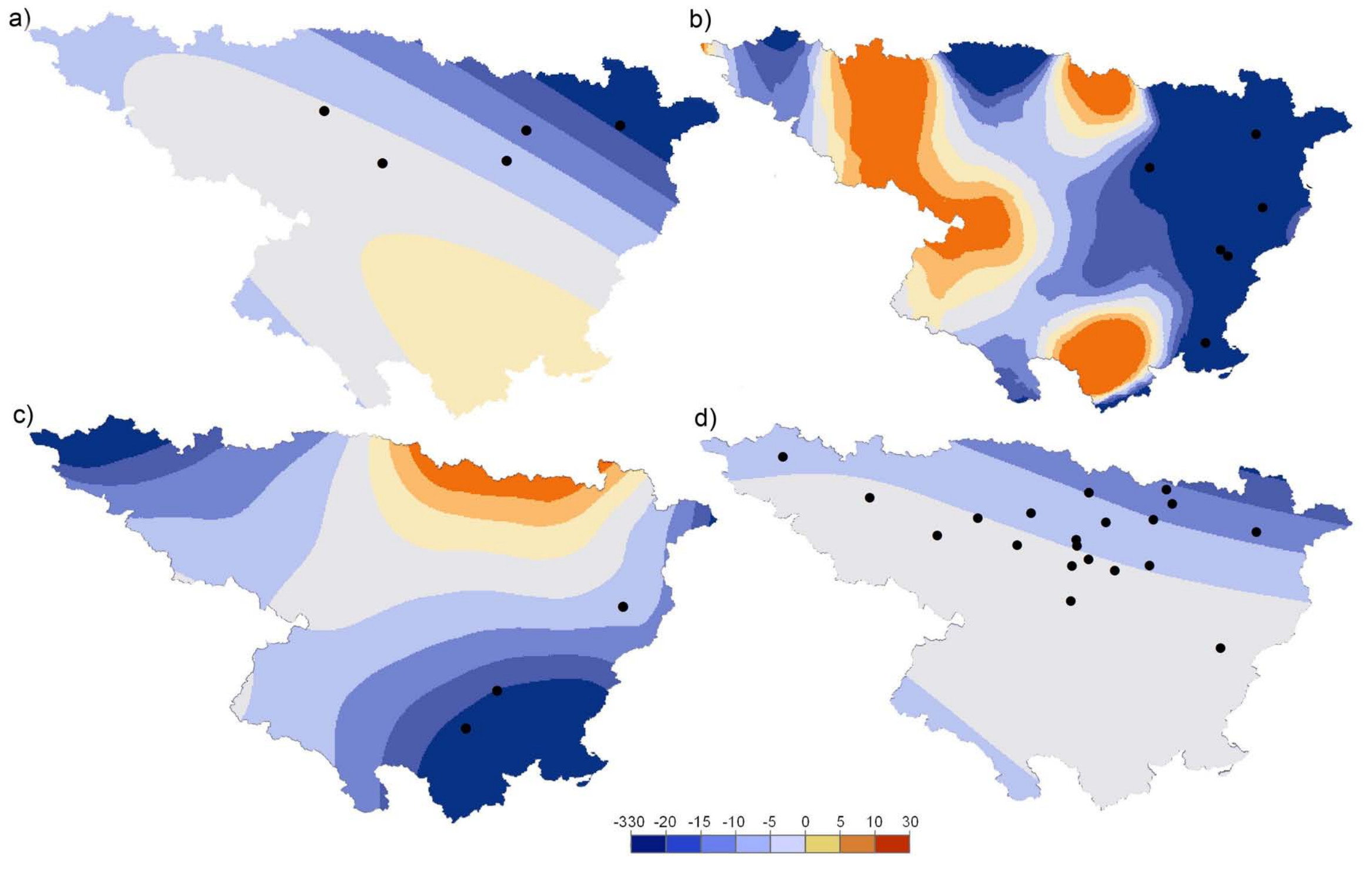
a)
b)
c)
d)
-330 -20 -15 -10 -5 0 5 10 30

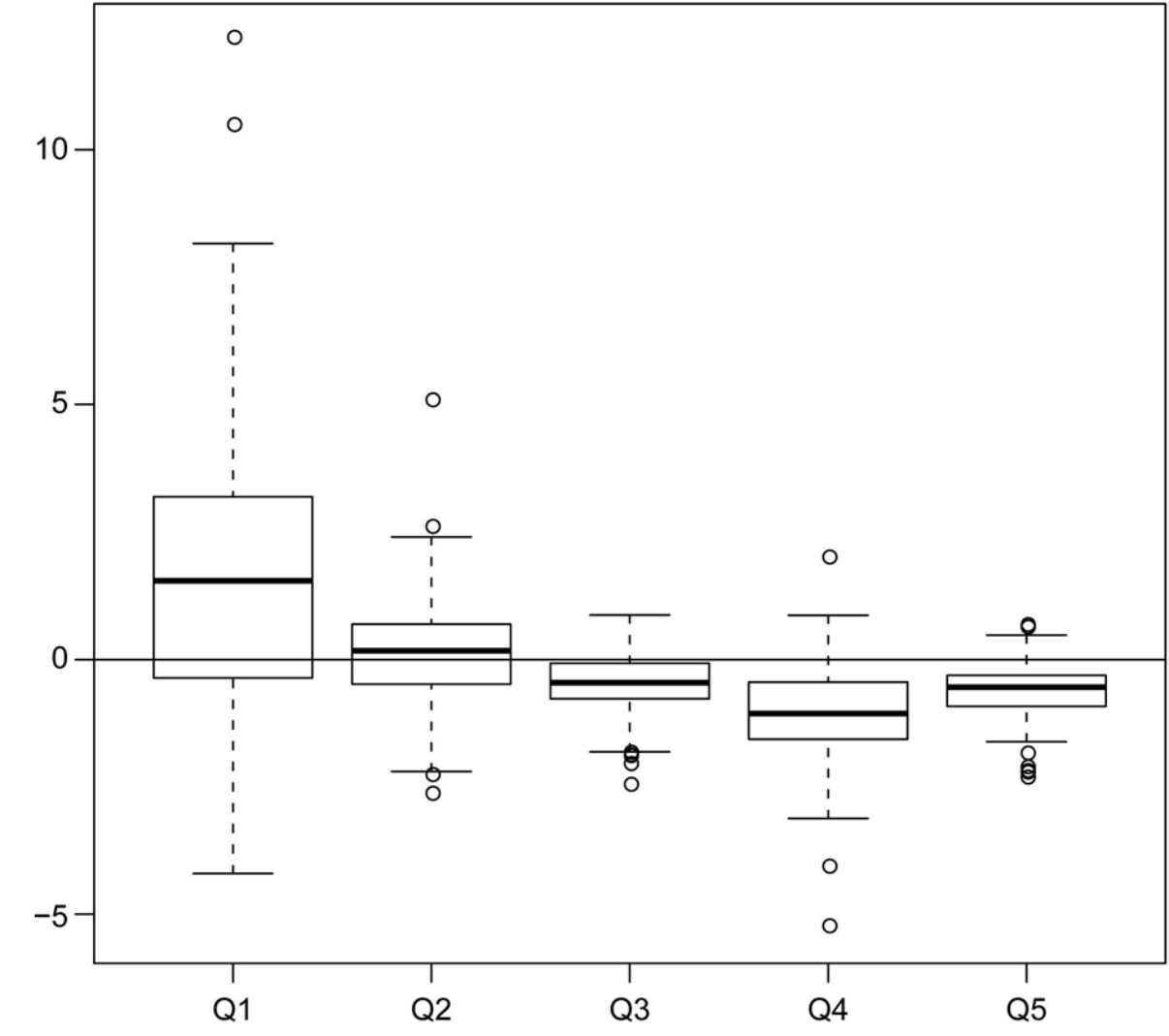
10
5
0
−5
Q1
Q2
Q3
Q4
Q5

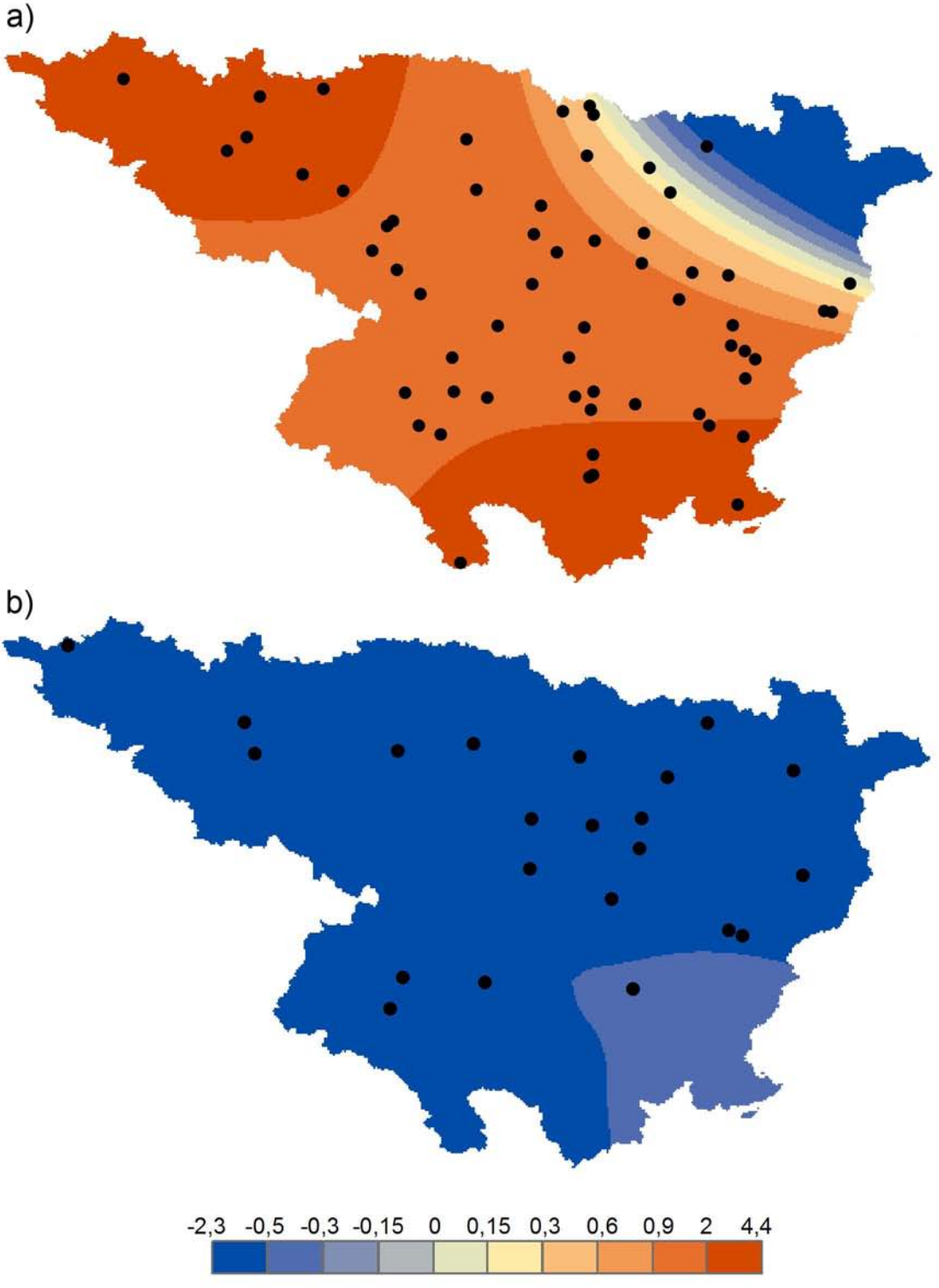
a)
b)
-2,3 -0,5 -0,3 -0,15 0 0,15 0,3 0,6 0,9 2 4,4

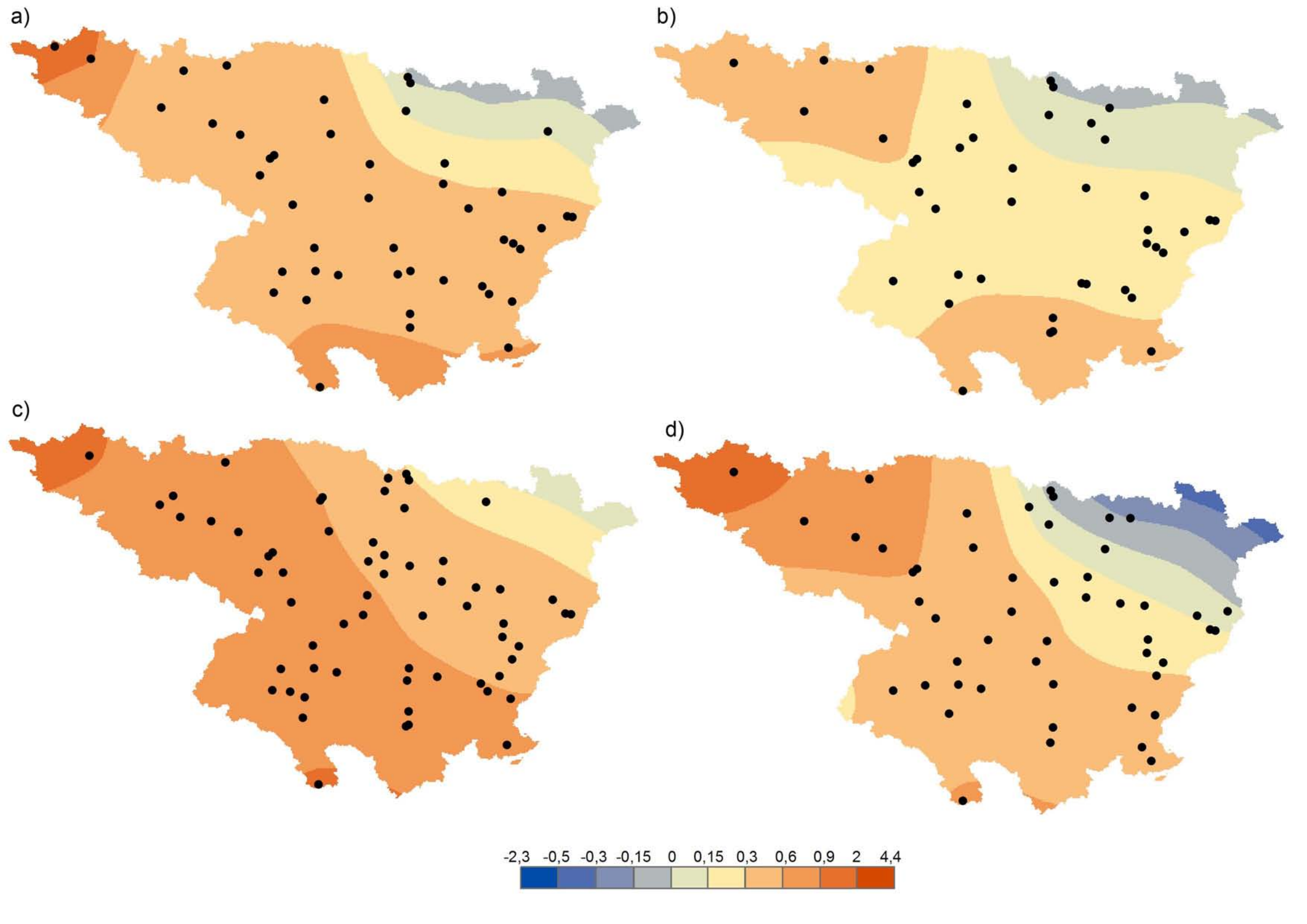
a)
b)
c)
d)
-2,3 -0,5 -0,3 -0,15 0 0,15 0,3 0,6 0,9 2 4,4

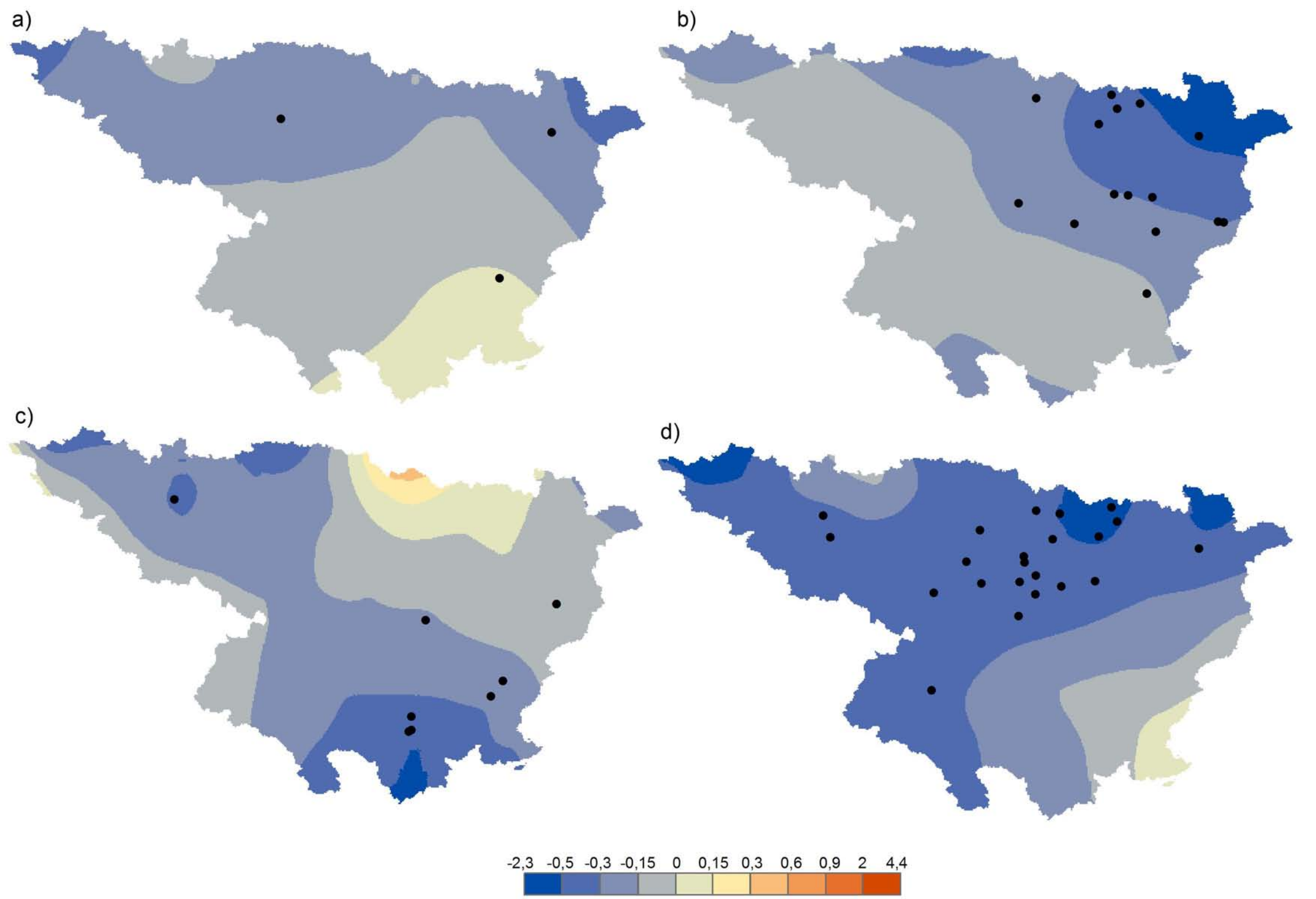
a)
b)
c)
d)
-2,3 -0,5 -0,3 -0,15 0 0,15 0,3 0,6 0,9 2 4,4

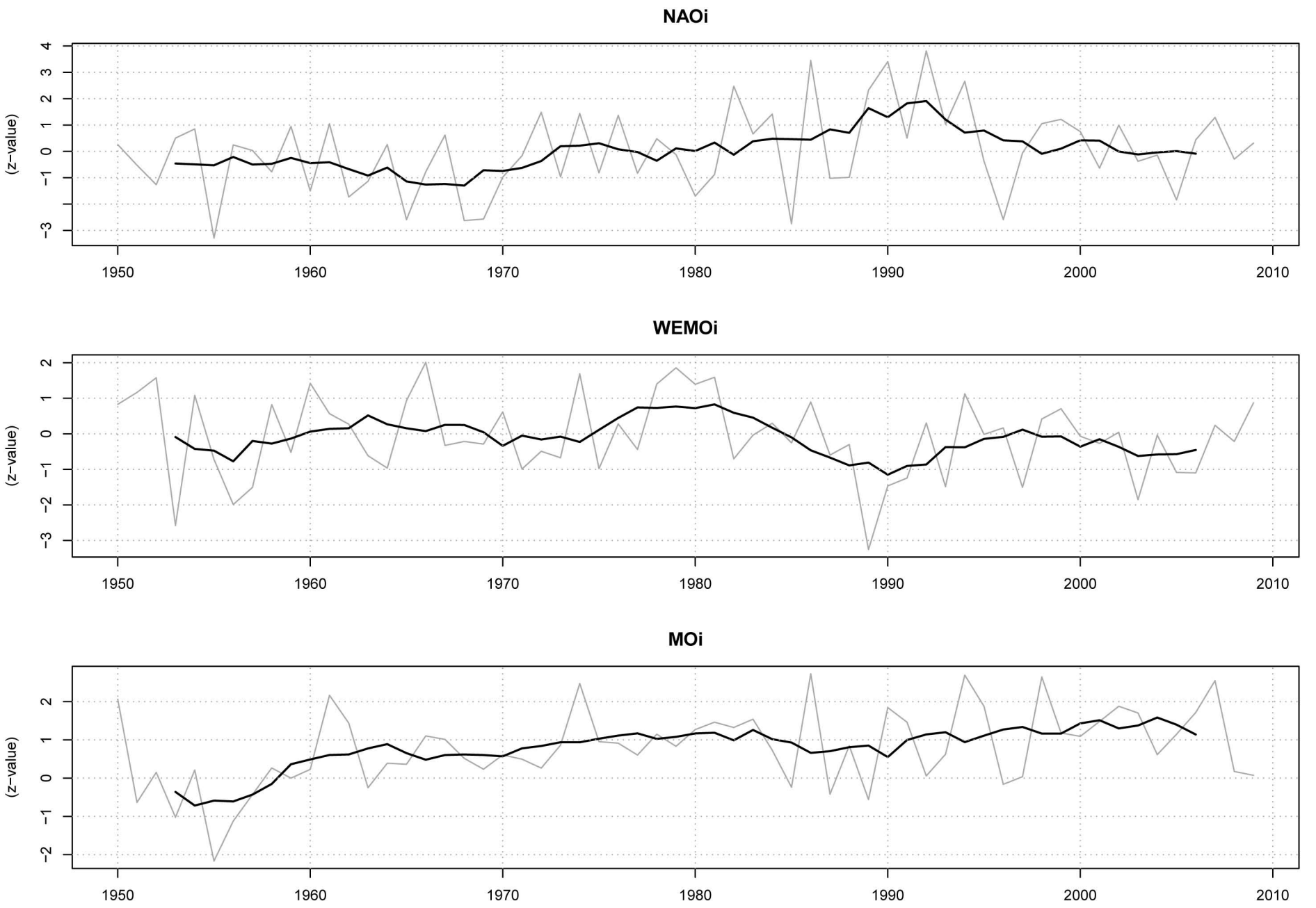
NAOi
(z−value)
4
3
2
1
0
−1
−3
1950
1960
1970
1980
1990
2000
2010
WEMOi
(z−value)
2
1
0
−1
−2
−3
1950
1960
1970
1980
1990
2000
2010
MOi
(z−value)
2
1
0
−1
−2
1950
1960
1970
1980
1990
2000
2010